JOC Article

Diels−Alder Reaction of Phosphaethene with 1,3-Dienes: An ab Initio Study

Chaitanya S. Wannere,[†] Raj K. Bansal,[‡,§] and Paul von Ragué Schleyer*[,†,§]

The Computational Chemistry Annex, Department of Chemistry, University of Georgia, Athens, Georgia 30602-2525, Department of Chemistry, University of Rajasthan, Jaipur 302 004, India, and Computer Chemie Centrum, Universität Erlangen-Nürnberg, Nägelsbachstrasse 25, 91052 Erlangen, Germany

schleyer@chem.uga.edu

Received August 4, 2002

Computations on Diels−Alder (DA) reactions of phosphaethene with 1,3-butadiene and with isoprene reveal asynchronous transition structures. The DFT (B3LYP/6-311+G**) activation energies of these reactions, 12−14 kcal/mol, are much lower than that of the parent ethene−butadiene reaction, 28 kcal/mol, even though the exothermicities of all lie in the same range, from −29 to −33 kcal/mol. The transition states (TSs) for the phosphethene−butadiene or isoprene DA reactions are earlier than the TSs of the butadiene−ethene cycloaddition. Due to the weakness of the C═P π bond compared to the C═C π bonds, the energies required to reach the phosphaethene TSs are much less than the carbocyclic cases. The computed ^{1}H NMR chemical shifts and nucleus independent chemical shifts (NICS) quantify the aromatic character of the transition states. Regioselectivities of the neutral phosphaethene−isoprene DA reactions are modest, at best. However, computations on radical cation DA reactions of phosphaethene with isoprene, which proceed stepwise with open chain intermediates, can account for the high regioselectivities that have been observed in some cases.

Introduction

The Diels−Alder (DA) reaction, perhaps the most widely used synthetic method for the construction of six-membered rings,[1] also has been central in the development of theoretical models of pericyclic reactions.[2] The availability of new classes of organophosphorus compounds with >C═P− functionalities, namely, phosphaalkenes,[3−7] heterophospholes,[6,8−10] anellated azaphospholes,[11−14] and phosphinines,[15] has further enlarged the scope of the DA reaction. A number of [4 + 2] cycloadditions have been carried out successfully using these phosphorus compounds, mostly as dienophiles, but in some cases as diene components as well. Unlike the phosphaalkenes, which have a strong tendency to undergo [2 + 2] dimerization unless bulky substituents are present,[3,5,16] the DA reaction of the parent phosphaethene, generated in situ, with 2,3-dimethyl-1,3-butadiene leads to a tetrahydrophosphinine.[17] Likewise, the behavior of the phosphabutadienes is governed by the nature of the substitutents: they may dimerize in the [2 + 2] mode[18] or may undergo [4 + 2] cycloadditions acting

* To whom the correspondence should be addressed.
† University of Georgia.
‡ University of Rajasthan.
§ Universität Erlangen−Nürnberg.

(1) (a) Diels, O.; Alder, K. *Ann*. **1928**, *460*, 98. (b) Woodward, R. B.; Katz, T. J. *Tetrahedron* **1959**, *5*, 70. (c) Onishchenko, A. S. *Diene Synthesis*; Israel Program for Scientific Translations: Jerusalem, 1964. (d) Huisgen, R.; Grashey, R.; Sauer, J. In *The Chemistry of Alkenes*; Patai, S., Ed.; Wiley: New York, 1964; p 739. (e) Wasserman, A. *Diels−Alder Reactions*; Elsevier: New York, 1965. (f) Sauer, J. *Angew. Chem., Int. Ed. Engl.* **1967**, *6*, 16. (g) Hamer, J. *1,4-Cycloaddition Reactions*; Academic Press: London, 1967.

(2) (a) Evans, M. G.; Warhurst. E. *Trans. Faraday Soc.* **1938**, *34*, 614. (b) Evans, M. G. *Trans. Faraday Soc.* **1939**, *35*, 824.

(3) Shvetsov-Shilovskii, N. I.; Bobkova, R. G.; Ignatova, N. P.; Melnikov, N. N. *Russian Chem. Rev*. **1977**, *46*, 514.

(4) Fluck, E. *Top. Phosphorous Chem*. **1980**, *10*, 193.

(5) (a) Apple, R.; Knoll, F.; Ruppert, I. *Angew. Chem., Int. Ed. Engl*. **1981**, *20*, 731. (b) Apple, R. *Pure Appl. Chem*. **1987**, *59*, 977. (c) Appel, R. In *Multiple Bonds and Low Coordination in Phosphorus Chemistry*; Regitz, M., Scherer, O. J., Eds.; Thieme: Stuttgart, **1990**, p 157.

(6) Weber, B.; Regitz, M. In *Methods in Organic Chemistry (Houben-Weyl)*; Regitz, M., Ed.; Thieme: Stuttgart, 1982; Vol. 4, Part E 1, p 27.

(7) Markovskii, L. N.; Romanenko, V. D. *Tetrahedron* **1989**, *45*, 6019.

(8) Schmidpeter, A.; Karaghiosoff, K. In *Rings, Clusters and Polymers of Main Group and Transition Elements*; Roesky, H. W., Ed.; Elsevier: Amsterdam, 1989; p 307.

(9) Schmidpeter, A.; Karaghiosoff, K. In *Multiple Bonds and Low Coordination in Phosphorus Chemistry*; Regitz, M., Scherer, O. J., Eds.; Thieme: Stuttgart, 1990; p 258.

(10) Schmidpeter, A. In *Comprehensive Heterocyclic Chemistry−II*; Katritzky, A. R., Rees, C. W., Sciven, E. F. V., Eds.; Pergamon: Oxford, 1996; Vol. 3, pp 709 and 715; Vol. 4, p 771.

(11) Bansal, R. K.; Karaghiosoff, K.; Schmidpeter, A. *Tetrahedron* **1994**, *50*, 7675. (b) Bansal, R. K.; Heinicke, J. *Chem. Rev*. **2001**, *101*, 3549.

(12) Bansal, R. K.; Karaghiosoff, K.; Gandhi, N.; Schmidpeter, A. *Synthesis* **1995**, 361.

(13) Bansal, R. K.; Mahnot, R.; Pandey, G.; Gupta, R. *J. Indian Chem. Soc*. **1995**, *71*, 415.

(14) Bansal, R. K.; Gupta, N.; Surana, A. *J. Indian Chem. Soc*. **1998**, *75*, 648.

(15) (a) Märkl, G. In *Methods in Organic Chemistry (Houben-Weyl)*; Regitz, M., Ed.; Thieme: Stuttgart, 1982; Vol. 4, Part E1, p 72. (b) Märkl, G. In *Multiple Bonds and Low Coordination in Phosphorus Chemistry*; Regitz, M., Scherer, O. J., Eds.; Thieme: Stuttgart, 1990; pp 220.

(16) Arbuzov, B. A.; Dianova, E. N. *Phosphorous Sulfur* **1986**, *26*, 203.

(17) Pellerin, B.; Guenot, P.; Denis, J.-M. *Tetrahedron Lett*. **1987**, *28*, 5811.

10.1021/jo026284i CCC: $22.00
Published on Web 11/28/2002

SCHEME 1

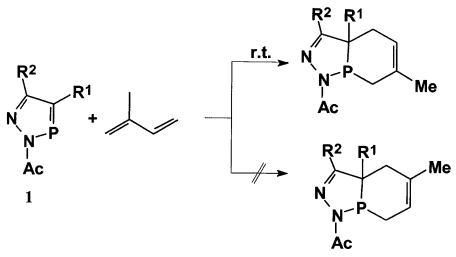

as dienophiles.[19] DA reactions involving the >C═P− functionality of a few heterophospholes have been reported.[8−10,16] In some cases, the phosphabutadiene system within the heterophosphole ring acts as a diene component.[20−22]

Remarkably, complete regioselectivity has been reported in the DA reaction of 2-acetyl-2*H*-1,2,3-diazaphosphole with isoprene (Scheme 1): "the other isomer was not detected" in the ^{31}P NMR signals of the product.[23] However, the analytical methods used to purify the products and limits of detectability were not mentioned in the reference. 1,3-Azaphospholo[5,1-*a*]isoquinoline undergoes DA reactions with 2,3-dimethyl-1,3-butadiene[24] and with isoprene;[25] 62−100% regioselectivity was observed in the latter case, depending on the conditions (Scheme 2). Experimentally, DA reactions of 1,3-azaphospholo[5,1-*b*]benzothiazoles,[26] 1,4,2-diazaphospholo-[5,4-*b*]benzothiazoles, thiazolines,[27] and 1,4,2-diazaphospholo[4,5-*a*]pyridines[28] with isoprene showed 70−100% regioselectivity (Scheme 3).

Many ab initio[29−32] and semiempirical [33−46] calculations on DA cycloadditions have been reported. The prototype DA cycloaddition of 1,3-butadiene with ethene has been computed theoretically at different levels, and a well-defined synchronous transition state, **TS$_1$**, has been established.[47] However, unsymmetrical reactants (e.g., isoprene, acrolein) involve asynchronous transition states, i.e., the lengths of two newly forming bonds differ significantly in the TS. Asynchronicity of such transition states has been established both by experimental[48] and by theoretical methods.[49−51]

In contrast, theoretical studies of DA reactions involving phosphorus and the aromaticity of their transition states are scarce. The DA cycloadditions of phospha-1,3-butadienes with ethene were computed to be very exothermic with low activation energies.[52] Ab initio investigations of the [2 + 4] cycloadditions of phosphaethene with 2*H*-phosphole[53] and with 1,3-butadiene[54−57] revealed such low activation energies and a preference for endo approach. It was concluded that the presence of phosphorus in a DA reactant lowers the activation energy relative to that of the hydrocarbon systems, due to the weakness of the C═P π bond compared to the C═C π bond.[52] We have now carried out ab initio calculations on the prototype DA reactions of phosphaethene with 1,3-butadiene and with isoprene at the B3LYP/6-311+G** DFT level to ascertain the nature of the transition states and to examine the regioselectivity. The aromaticity of the transition states has been established by computations of the ^{1}H NMR chemical shifts,[58] the magnetic susceptibility exaltations,[59] and the NICS[60] values. DA reactions of isoprene with phosphaethene and related systems, proceeding through a concerted TS, show no appreciable regioselectivity. Alternatively, we show that

(18) Martin, G.; Ocando-Mavarez, E. *Heteroat. Chem*. **1991**, *2*, 651.
(19) Apple, R.; Knoch, F.; Kunze, H. *Chem. Ber*. **1984**, *117*, 3151.
(20) Märkl, G.; Lieb, F.; Martin, C. *Tetrahedron Lett*. **1971**, 1249.
(21) Kobayashi, Y.; Fujino, Sh.; Kumadaki, I. *J. Am. Chem. Soc*. **1981**, *103*, 2645.
(22) (a) Karaghiosoff, K.; Klehr, H.; Schmidpeter, A. *Chem. Ber*. **1986**, *199*, 410. (b) Schmidpeter, A.; Klehr, H. *Z. Naturforsch., B: Chem. Sci*. **1983**, *38*, 1484.
(23) Chen, R.; Cai, B.; Li, G. *Synthesis* **1991**, 783.
(24) Bansal, R. K.; Hemrajani, L.; Gupta, N. *Heteroat. Chem*. **1999**, *10*, 598.
(25) Bansal, R. K.; Jain, V. K.; Gupta, N.; Gupta, Nidhi, Hemrajani, L.; Baweja, M.; Jones, P. G. *Tetrahedron* **2002**, *58*, 1573.
(26) Karaghiosoff, K.; Hackenbracht, G.; Schmidpeter, A.; Bansal, R. K.; Gupta, N.; Sharma, D. C.; Mahnot, R.; Kabra, V. *Phosphorous Sulfur Silicon* **1993**, *77*, 235.
(27) Bansal, R. K.; Gupta, N.; Gandhi, N.; Karaghiosoff, K. Results to be published.
(28) Karaghiosoff, K.; Cleve, C.; Schmidpeter, A. *Phosphorous Sulfur* **1986**, *28*, 289.
(29) Townshend, R. E.; Ramunni, G.; Segal, G.; Hehre, W. J.; Salem, L. *J. Am. Chem. Soc*. **1976**, *98*, 2190.
(30) Bernardi, F.; Bottomi, A.; Robb, M. A.; Field, M. J.; Hillier, I. H.; Guest, M. F. *J. Chem. Soc., Chem. Commun*. **1985**, 1051.
(31) Burke, L. A. *Int. J. Quant. Chem*. **1986**, *29*, 511.
(32) (a) Houk, K. N.; Lin, Y.-T.; Brown, F. K. *J. Am. Chem. Soc*. **1986**, *108*, 554. (b) Beno, B. R.; Houk, K. N.; Singleton, D. A. *J. Am. Chem. Soc*. **1996**, *118*, 9984. (c) Sakai, S. *J Phys. Chem*. **2000**, *104*, 922.
(33) Kikuchi, O. *Tetraheron* **1971**, *27*, 2791.
(34) McIver, J. W., Jr. *Acc. Chem. Res*. **1974**, *7*, 72.
(35) Dewar, M. J. S.; Griffin, A. C.; Kirschner, S. *J. Am. Chem. Soc*. **1974**, *96*, 6225.
(36) Basilevsky, M. V.; Shamov, A. G.; Tikhomirov, V. A. *J. Am. Chem. Soc*. **1977**, *99*, 1369.
(37) Dewar, M. J. S.; Olivella, S.; Rzepa, H. S. *J. Am. Chem. Soc*. **1978**, *100*, 5650.
(38) Pancir, J. *J. Am. Chem. Soc*. **1982**, *104*, 7424.
(39) Dewar, M. J. S.; Pierini, A. B. *J. Am. Chem. Soc*. **1984**, *106*, 203.
(40) Dewar, M. J. S. *J. Am. Chem. Soc*. **1984**, *106*, 209.
(41) Dewar, M. J. S.; Olivella, S.; Stewart, J. J. P. *J. Am. Chem. Soc*. **1986**, *108*, 5771.
(42) Dewar, M. J. S.; Zoebisch, E. G.; Healy, E. F.; Stewart, J. J. P. *J. Am. Chem. Soc*. **1985**, *107*, 3902.
(43) Doi, T.; Shimizu, K.; Takahashi, T.; Tsuji, J.; Yamamoto, K. *Tetrahedron Lett*. **1990**, *31*, 3313.
(44) Takahashi, T.; Sakamoto, Y.; Doi, T. *Tetrahedron Lett*. **1992**, *33*, 3519.
(45) Marshall, J. A.; Grote, J.; Audia, J. E. *J. Am. Chem. Soc*. **1987**, *109*, 1186.
(46) Eksterowicz, J. E.; Houk, K. N. *Chem. Rev*. **1993**, *93*, 2439.
(47) (a) Brown, F. K.; Houk, K. N. *Tetrahedron Lett*. **1984**, *25*, 4609. (b) Houk, K. N.; González, J.; Li, Y. *Acc. Chem. Res*. **1995**, *28*, 81. (c) Wiest, O.; Houk, K. N.; Black, K. A.; Thomas, B., IV. *J. Am. Chem. Soc*. **1995**, *117*, 8594. (d) Wiest, O.; Houk, K. N. *Top. Curr. Chem*. **1996**, *183*, 1. (e) Houk, K. N.; Beno, B. R.; Nendel, M.; Black, K.; Yoo, H. Y.; Wilsey, S.; Lee, J. K. *J. Mol. Struct. (THEOCHEM)* **1997**, *398−399*, 169.
(48) Gajewski, J. J.; Peterson, K. B.; Kagel, J. R. *J. Am. Chem. Soc*. **1987**, *109*, 5545.
(49) Woodward, R. B.; Katz, T. J. *Tetrahedron* **1959**, *5*, 70.
(50) (a) Brown, F. K.; Houk, K. N.; Burnell, D. J.; Valenta, Z. *J. Org. Chem*. **1987**, *52*, 3050. (b) Brown, F. K.; Houk, K. N. *Tetrahedron Lett*. **1985**, *26*, 2297.
(51) Loncharich, R. J.; Brown, F. K.; Houk, K. N. *J. Org. Chem*. **1989**, *54*, 1129.
(52) Bachrach, S. M.; Liu, M. *J. Org. Chem*. **1992**, *57*, 6736.
(53) Salzner, U.; Bachrach, S. M.; Mulhearn, D. C. *J. Comput. Chem*. **1997**, *18*, 198.
(54) Lee, B.-Su; Kim, C. K.; Choi, J. W.; Lee, I. *Bull. Korean Chem. Soc*. **1996**, *17*, 849; *Chem. Abstr*. **1996**, *125*, 327857.
(55) Mulhearn, D. C.; Bachrach, S. M. *Proceedings of the First Electron. Comput. Chem. Conf*erence; Paper 11; *Chem. Abstr*. **1994**, *124*, 316229.
(56) Penkovsky, V.; Kharchenko, V.; Alexeiko, L. *Phosphorus Sulfur Silicon Relat. Elem*. **1993**, *77*, 81.
(57) Schoeller, W. W. *J. Chem. Soc., Chem. Commun*. **1985**, 334.
(58) The expected absolute proton shieldings, σ, were converted to chemical shifts, δ, as the difference from proton shieldings of TMS, 31.31 ppm.

SCHEME 2

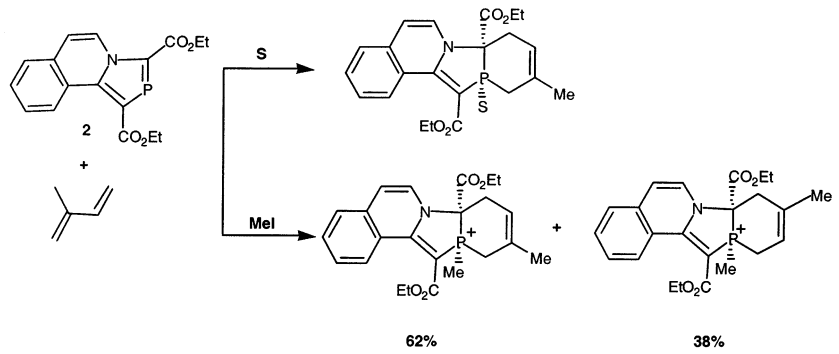

SCHEME 3

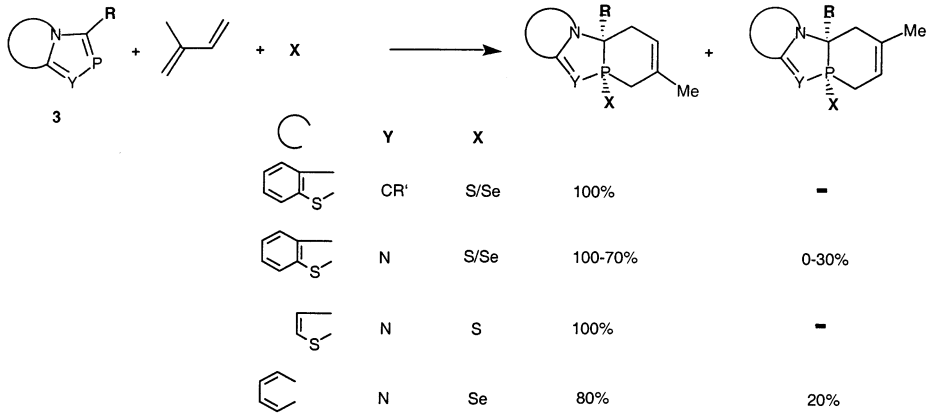

reactions proceeding through radical cation mechanisms can give products with high regioselectivity.

Some pericyclic reactions may be prohibitively slow or may not give the desired products. Lewis acids or catalytic agents may assist by complexation, thereby reducing the electron density of one reactant. Alternatively, one electron may be removed from the system by an oxidizing agent; this may accelerate the reaction.[61] This approach has been termed as "hole catalysis" by Bauld.[62] Radical cation reactions, which do not need to be electrocyclic, generally have low activation energies but nevertheless show high degrees of regio- and stereoselectivity.[63] Radical cation reactions thus complement neutral reactions. DA reactions of ethene with butadiene radical cation have recently been investigated theoretically.[64] A stepwise addition involving open chain intermediates but leading to a DA-like product, cyclohexene radical cation, was found to have a total activation barrier of only 6.3 kcal/mol and exothermicity of 45.6 kcal/mol.[64] All the TSs and intermediates were found to have lower energies than the separated starting reactants.

We have now investigated, similarly, the stepwise reaction of the isoprene radical cation with phosphaethene with density functional theory at the UB3LYP/6-311+G** level. A reaction pathway leading to the radical cation DA products was shown to be possible.

Computational Methods

All results were obtained with the Gaussian 94[65] and Gaussian 98[66] series of programs. Reactants and products as well as transtion structures resulting from the Diels−Alder reaction of phosphaethene with 1,3-dienes were optimized initially at HF/6-31G* and finally at the B3LYP/6-311+G** DFT level. The frequencies were computed at B3LYP/6-31G*; the transition structures were confirmed by the presence of one imaginary frequency. Unscaled zero point energy correc-

(59) (a) Keith, T. A.; Bader, R. F. W. *Chem. Phys. Lett.* **1993**, *210*, 223. (b) Cheeseman, J. R.; Frisch, M. J.; Trucks G. W.; Keith, T. A. *J. Chem. Phys.* **1995**, *104*, 5497. (c) Wolinski, K.; Hilton, J. F.; Pulay, P. *J. Am. Chem. Soc.* **1990**, *112*, 8251.

(60) (a) Schleyer, P. v. R.; Maerker, C.; Dransfeld, A.; Jiao, H.; Hommes, N. J. R. v. E. *J. Am. Chem. Soc.* **1996**, *118*, 6317. (b) Schleyer, P. v. R.; Jiao, H.; Hommes, N. J. R. v. E.; Malkin, V. G.; Malkina, O. L. *J. Am. Chem. Soc.* **1997**, *119*, 12669. (c) Schleyer, P. v. R.; Manoharan, M.; Wang, Z. X.; Kiran, B.; Jiao, H.; Puchta, R.; Hommes, N. J. R. v. E. *Org. Lett.* **2001**, *3*, 2465.

(61) Müller, F.; Mattay, J. *Chem. Rev.* **1993**, *93*, 99.

(62) Bauld, N. L. *J. Am. Chem. Soc.* **1992**, *114*, 5800.

(63) Schmittel, M.; Wöhrle, C.; Bohn, I. *Chem. Eur. J.* **1996**, *2*, 1031.

(64) (a) Hofmann, M.; Schaefer, H. F. *J. Am. Chem. Soc.* **1999**, *121*, 6719. (b) Hofmann, M.; Schaefer, H. F. *J. Phys. Chem.* **1999**, *103*, 8895. (c) Hofmann, M.; Schaefer, H. F. *THEOCHEM* **2001**, *599*, 95.

(65) Frisch, M. J.; Trucks, G. W.; Schlegel, H. B.; Gill, P. M. W.; Johnson, B. G.; Robb, M. A.; Cheeseman, J. R.; Keith, T.; Petersson, G. A.; Montgomery, J. A.; Raghavachari, K.; Al-Laham, M. A.; Zakrzewski, V. G.; Ortiz, J. V.; Foresman, J. B.; Cioslowski, J.; Stefanov, B. B.; Nanayakkara, A.; Challacombe, M.; Peng, C. Y.; Ayala, P. Y.; Chen, W.; Wong, M. W.; Andres, J. L.; Replogle, E. S.; Gomperts, R.; Martin, R. L.; Fox, D. J.; Binkley, J. S.; Defrees, D. J.; Baker, J.; Stewart, J. P.; Head-Gordon, M.; Gonzalez, C.; Pople, J. A. *Gaussian 94*, revision E.2; Gaussian, Inc.: Pittsburgh, PA, 1995.

(66) Frisch, M. J.; Trucks, G. W.; Schlegel, H. B.; Scuseria, G. E.; Robb, M. A.; Cheeseman, J. R.; Zakrzewski, V. G.; Montgomery, J. A., Jr.; Stratmann, R. E.; Burant, J. C.; Dapprich, S.; Millam, J. M.; Daniels, A. D.; Kudin, K. N.; Strain, M. C.; Farkas, O.; Tomasi, J.; Barone, V.; Cossi, M.; Cammi, R.; Mennucci, B.; Pomelli, C.; Adamo, C.; Clifford, S.; Ochterski, J.; Petersson, G. A.; Ayala, P. Y.; Cui, Q.; Morokuma, K.; Malick, D. K.; Rabuck, A. D.; Raghavachari, K.; Foresman, J. B.; Cioslowski, J.; Ortiz, J. V.; Stefanov, B. B.; Liu, G.; Liashenko, A.; Piskorz, P.; Komaromi, I.; Gomperts, R.; Martin, R. L.; Fox, D. J.; Keith, T.; Al-Laham, M. A.; Peng, C. Y.; Nanayakkara, A.; Gonzalez, C.; Challacombe, M.; Gill, P. M. W.; Johnson, B. G.; Chen, W.; Wong, M. W.; Andres, J. L.; Head-Gordon, M.; Replogle, E. S.; Pople, J. A. *Gaussian 98*, revision A.5; Gaussian, Inc.: Pittsburgh, PA, 1998.

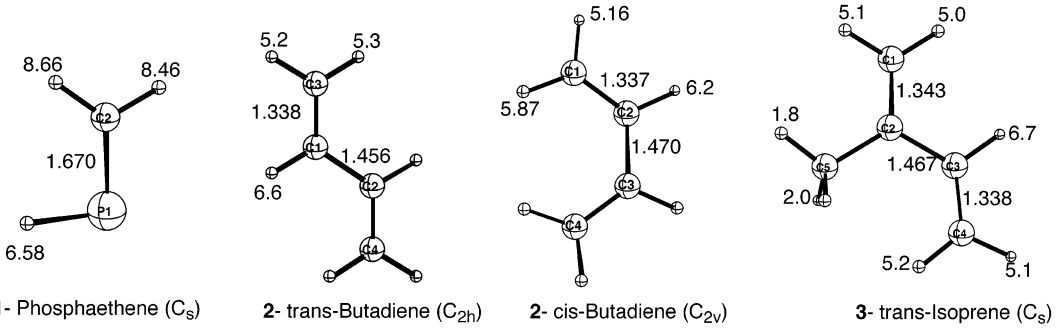

FIGURE 1. Bond lengths (B3LYP/6-311+G**) and ^{1}H NMR chemical shifts (GIAO-B3LYP/6-31+G*//B3LYP/6-311+G**, in δ ppm) of reactants.

tions (ZPE) from the same level were applied to the B3LYP/6-311+G** energies. The potential energy surface along the reaction course(s) for the parent as well as phosphaethene and butadiene DA reaction is computed at B3LYP/6-311+G**. The absolute energies and ZPE values of all the structures are reported in Supporting Information. The bond orders, of the various bonds, in TSs were evaluated using the NBO program[67] as implemented in the Gaussian 98 package.

For the radical cation reactions, the geometries of all reactants, intermediates, TSs, and products were optimized with 6-31G* and 6-311+G** basis sets and Becke's three-parameter hybrid functional in conjunction with the correlation functional of Lee, Yang, and Parr (UB3LYP) as implemented in Gaussian 98. The frequencies were computed at UB3LYP/6-31G* and unscaled zero point corrections from the same level were applied to the UB3LYP/6-311+G** energies. The absolute energies, ZPE values, and geometries of reactants and products are given in Supporting Information.

The magnetic susceptibilities were computed by the CSGT method[59a,b] at B3LYP/6-31+G*//B3LYP/6-311+G**. NICS values were obtained at GIAO-B3LYP/6-31+G*//B3LYP/6-311+G**.[59c] Dissected NICS[60] and proton chemical shifts[58] were evaluated using the deMon-Master NMR program,[68] at the SOS-DFPT[69] level with the Perdew-Wang-91(PW91)[70a,b] exchange correlation functional and the IGLO-III TZ2P basis set[70c] (recommended options).

Results and Discussion

The first part of the study involved the parent and six other DA reactions, as summarized in Table 1.

Geometries. The B3LYP/6-311+G**-optimized geometries of the reactants, phosphaethene (**1**), 1,3-butadiene (**2**), and isoprene (**3**) (Figure 1), and the products (**4**−**9**) (Figure 2), as well as the transition structures, $\mathbf{TS_1}$ and $\mathbf{TS_2}$−$\mathbf{TS_7}$ (Figure 3), show the change in bond lengths along the reaction course.

TABLE 1. Activation Energies[a] (ΔE_a, kcal/mol) and Exothermicities[a] (ΔE_{rxn}, kcal/mol) for Reactions 1−7 between Phosphaethene (1) and 1,3-Dienes (2 and 3)

reaction no.	reaction	ΔE_a	ΔE_{rxn}
1	butadiene+ ethene → $\mathbf{TS_1}$	28.00	−29.19
2	**1** (endo) + **2** → $\mathbf{TS_2}$ → **4**	12.41	−29.71
3	**1** (exo) + **2** → $\mathbf{TS_3}$ → **5**	14.48	−32.15
4	**1** (endo) + **3** → $\mathbf{TS_4}$ → **6** (1:4 P/Me)	12.46	−30.84
5	**1** (endo) + **3** → $\mathbf{TS_5}$ → **7** (1:3 P/Me)	12.30	−31.01
6	**1** (exo) + **3** → $\mathbf{TS_6}$ → **8** (1:4 P/Me)	14.47	−33.11
7	**1** (exo) + **3** → $\mathbf{TS_7}$ → **9** (1:3 P/Me)	14.12	−33.03

[a] Relative energies at B3LYP/6-311+G** + ZPE (B3LYP/6-31G*).

The computed lengths of the P−C double bond in **1** (1.67 Å) and the P−C single bond in **4**−**9** (1.86−1.89 Å) are very close to the experimental values of related compounds.[5c,71] The P−C bond lengths in the phosphaethene moiety in the transition structures $\mathbf{TS_2}$−$\mathbf{TS_7}$ (∼1.71 Å) are intermediate between C=P and C−P bond lengths. The central C−C bonds of 1,3-butadiene (1.47 Å) and of isoprene (1.48 Å) shorten upon reaction with phosphaethene (∼1.40 Å in $\mathbf{TS_2}$−$\mathbf{TS_7}$) and become typical C−C double bonds (∼1.33 Å) in the products. The newly forming, C1−C6, bond lengths in $\mathbf{TS_2}$−$\mathbf{TS_7}$ are slightly longer (∼0.1−0.2 Å) than those in the prototype ethene−butadiene DA cycloaddition $\mathbf{TS_1}$. Although the two newly forming bonds, P−C and C−C in $\mathbf{TS_2}$−$\mathbf{TS_7}$, do not differ significantly in their lengths in the transition structures, the P−C bonds (∼1.88 Å) are, as expected, longer than the C−C bonds (∼1.53 Å) in the products. Furthermore, P−C bonds are slightly longer in the exo approach transition structures relative to those from the endo approach transition structures.

While phosphaethene is planar, the 4-phosphacyclohexene rings in products **4**−**9** are puckered. The C−C=C−C substructures of these rings are almost planar, with dihedral angles of 0.6−1.2°, but there is considerable folding involving phosphorus. The C3−C4−P5−C6 dihedral angle, for example, is 39.9° in **4**. The C−P−C angle in **4** is 99.1°, which is in conformity with the usual small angles at phosphorus in rings.[8,72,73] In the transition

(67) (a) Carpenter, J. E.; Weinhold, F. *J. Mol. Struct. (THEOCHEM)* **1988**, *169*, 41. (b) Foster, J. P.; Weinhold, F. *J. Am. Chem. Soc.* **1980**, *102*, 7211. (c) Reed, A. E.; Weinhold, F. *J. Chem. Phys.* **1983**, *78*, 4066. (d) Reed, A. E.; Weinhold, F. *J. Chem. Phys.* **1983**, *78*, 1736. (e) Reed, A. E.; Weinstock, R. B.; Weinhold, F. *J. Chem. Phys.* **1985**, *83*, 735. (f) *NBO*, version 3.1: Glendening, E. D.; Reed, A. E.; Carpenter, J. E.; Weinhold, F. Theoretical Chemistry Institute, University of Wisconsin, Madison, 1996.

(68) (a) St-Amant, A.; Salahub, D. R. *Chem. Phys. Lett.* **1990**, *169*, 387. (b) Godbout, N.; Salahub, D. R.; Andzelm, J.; Wimmer, E. *Can. J. Chem.* **1992**, *70*, 560. (c) Salahub, D. R.; Fournier, R.; Mlynarsky, P.; Papai, I.; St- Amant, A.; Ushio, J. In *Density Functional Methods in Chemistry*; Labanowsky, J. Andzelm, J., Eds.; Springer: New York, 1991; pp 77.

(69) (a) Malkin, V. G.; Malkina, O. L.; Casida, M. E.; Salahub, D. R. *J. Am. Chem. Soc.* **1994**, *116*, 5898. (b) Malkin, V. G.; Malkina, O. L.; Eriksson, L. A.; Salahub, D. R. In *Modern Density Functional Theory*; Seminario, J. M., Politzer, P., Eds.; Elsevier: Amsterdam, 1995, p 273.

(70) (a) Perdew, J. P.; Wang, Y. *Phys. Rev. B* **1992**, *45*, 13244. (b) Perdew, J. P.; Chevary, J. A.; Vosko, S. H.; Jackson, K. A.; Pederson, M. R.; Singh, D. J.; Fiolhais, C. *Phys. Rev. B* **1992**, *46*, 6671. (c) Kutzelnigg, W.; Fleisher, U.; Schindler, M. In *NMR−Basic Principles and Progress*; Spinger: Heidelberg, 1990; Vol. 23, p 165.

(71) Hopkinson, M. J.; Kroto, H. W.; Nixon, J. F.; Simmons, N. P. C. *J. Chem. Soc., Chem. Commun.* **1976**, 513.

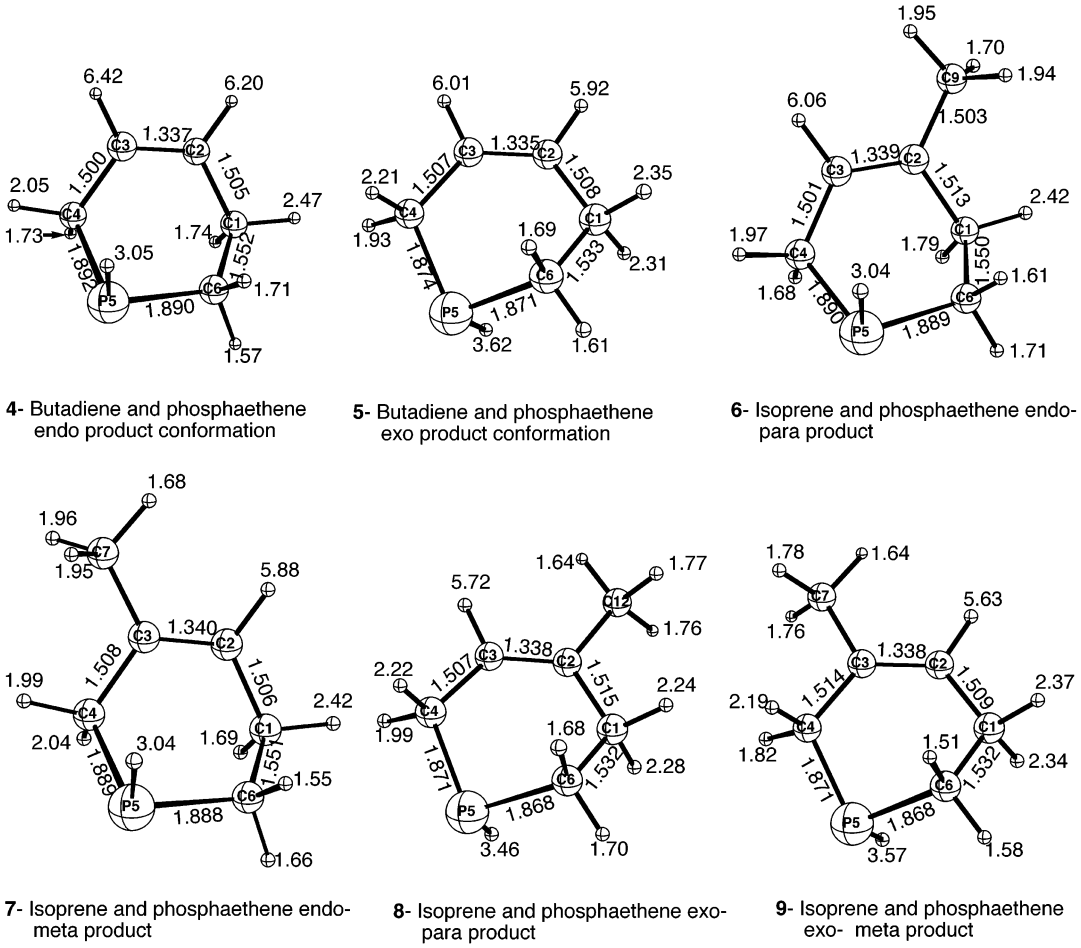

FIGURE 2. Geometries (B3LYP/6-311+G**) and ^{1}H chemical sifts in ppm (GIAO−B3LYP/6-31+G*//B3LYP/6-311+G**) of products of reactions of phosphaethene with 1,3-butadiene and with isoprene.

states, the phosphaethene and diene fragments approach each other in distinctly nonparallel planes, although the values of the C2−C3−P5−C6 dihedral angles are small, e.g., 6.5° in **TS$_2$** and 5.0° **TS$_5$**. The diene moieties in the transition structures (**TS$_2$**−**TS$_7$**) are nearly planar, and the C−C−C−C dihedral angle is close to zero.

Energies. The activation (ΔE_a) and reaction (ΔE_{rxn}) energies of reactions 1−7 are given in Table 1. While the exothermicities of DA reactions of ethene with 1,3-butadiene and with phosphabutadienes, reported earlier,[52] are quite similar, the ΔE_a values for the latter are smaller. Our results are parallel: the presence of phosphorus in the dienophile lowers the activation barriers (which range from 12.3 to 14.5 kcal/mol) for reactions 2−7, as compared to ΔE_a for the prototype ethene−butadiene cycloaddition, but the ΔE_{rxn} values (Table 1) are in the same range. The difference in ΔE_a between the carbocyclic and phospha DA reactions has been attributed to the weakness[74] of the C=P π bond relative to the C=C π bond.

The bond orders (Scheme 4) of the synchronous **TS$_1$** for the parent DA reaction as well as for asynchronous **TS$_2$**−**TS$_7$** show that the extent of double-bond formation on C2−C3 is greater in **TS$_1$**. Also, the extent of bond formation between C1−C6 and C4−C5 is somewhat larger in **TS$_1$** as compared to that between C1−C6 and C4−P5 in **TS$_2$**−**TS$_7$**. Consequently, the TSs for phosphaethene−butadiene or isoprene DA reactions are "earlier" than the **TS$_1$** of ethene−butadiene cycloaddition, (Figure 4; the reaction course "s" is defined as $s = (d_R - d)/(d_R - d_p)$, where d is the distance between C_1-C_4 and C_5-C_6 midpoints and d_R and d_p are the respective distances in the optimized reactant and product geometries). Hence, the energy necessary for reorganization of all bonds in reactions 2−7 is less than that needed in reaction 1. Since C−P π bonds are weaker than C−C π bonds,[74] the C=P bond reorganization energy also is less than that for C=C. Hence, ΔE_a is smaller for reactions 2−7 than for reaction 1. Also, note the smaller HOMO−LUMO gap between diene and phosphaethene (the FMO gap between butadiene and ethene is 6.26 e.v., and that between butadiene and phosphaethene is only 4.35 e.v.). Hence, on the basis of FMO theory, DA reactions 2−7 should be faster and occur with lower activation barriers than reaction 1.

On going from reactants to product in the parent DA reaction, two C=C bonds are converted into four C−C

(72) (a) Bachrach, S. M. *J. Phys. Chem.* **1989**, *93*, 7780. (b) Bachrach, S. M. *J. Org. Chem.* **1991**, *56*, 2205.
(73) Roush, W. K.; Gillis, H. R.; Ko, A. I. *J. Am. Chem. Soc.* **1982**, *104*, 2269.
(74) (a) Wiberg, K. B.; Nakaji, D. *J. Am. Chem. Soc.* **1993**, *115*, 10658. (b) Schleyer, P. v. R.; Kost, D. *J. Am. Chem. Soc.* **1988**, *110*, 2105. (c) Schmidt, M. W.; Truong, P. N.; Gordon, M. S. *J. Am. Chem. Soc.* **1987**, *109*, 5217.

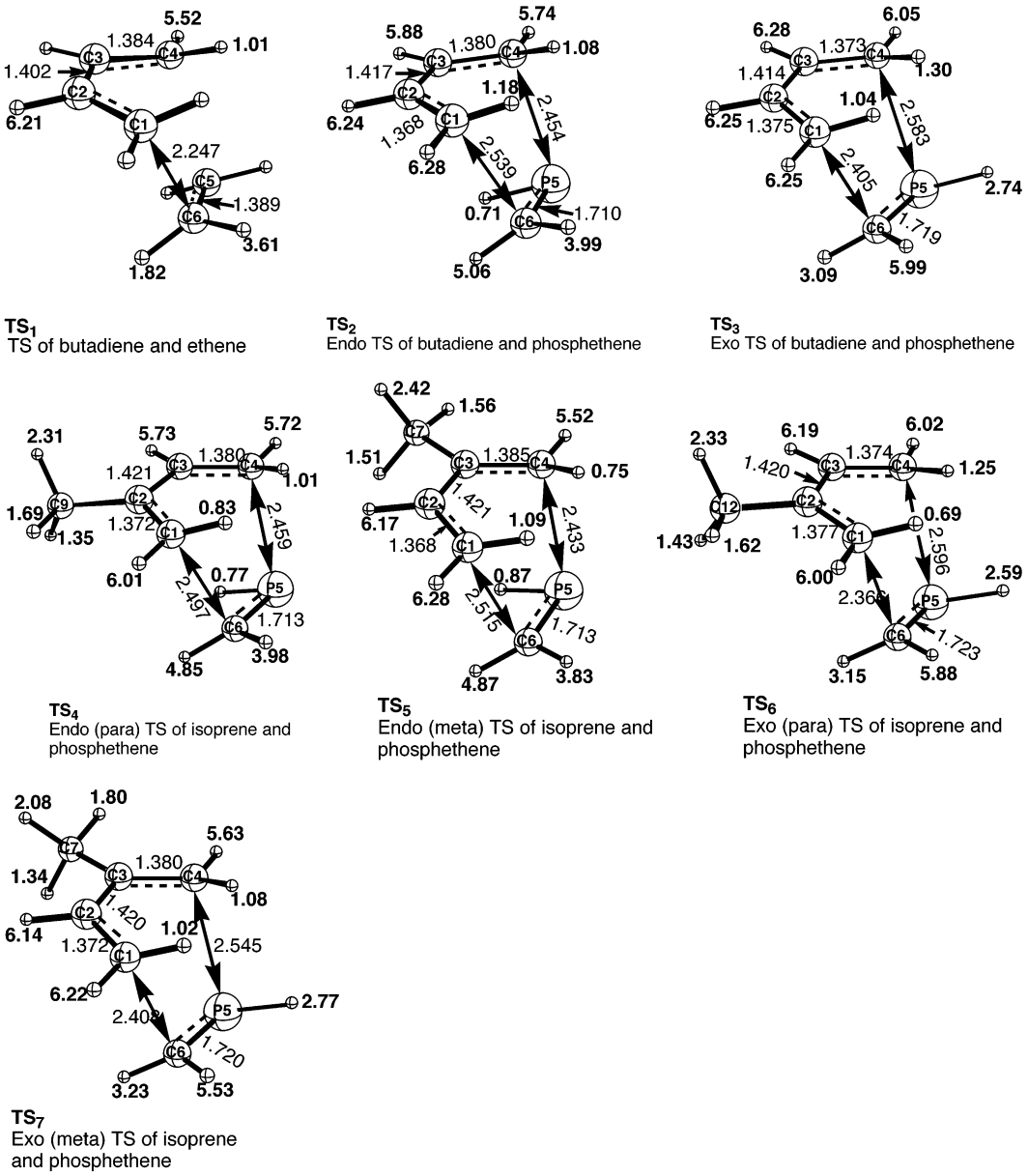

FIGURE 3. Bond lengths (B3LYP/6-311+G**, in Å) and ^{1}H NMR chemical shifts as well as NICS(GIAO-B3LYP/6-31+G*//B3LYP/6-311+G**, in ppm) of the transition states obtained in DA reactions of phosphaethene with butadiene, **TS$_2$** and **TS$_3$**, and isoprene, **TS$_4$**, **TS$_5$**, **TS$_6$**, and **TS$_7$**. In all of the TSs, C2−C3−P5−C6 are in one plane. Dotted lines denote the mobile electron localization as given by the dissected NICS (IGLO method) computations.

bonds. An estimate of the exothermicity, via bond energies (obtained from ref 74b), gives an enthalpy of −37.8 kcal/mol. A similar estimate for the phosphaethene−butadiene or isoprene system gives an exothermicity of −35.7 kcal/mol. The exothermicities of reaction 1 and of reactions 2−7, evaluated via bond energies, are in close agreement, as are the ΔE_{rxn} values in Table 1.

Stereoselectivity and Regioselectivity. The ∼2 kcal/mol lower activation energies for reactions 2, 4, and 5 indicate that the approach of the reactants with an endo P−H group is kinetically more favorable than attack with an exo P−H. A similar effect was noted in the DA reactions of ethene with 1-phosphabutadienes.[52] The preference for the endo transition state, in our cases, is due to the orientation of the phosphorus lone pair away from the butadiene. Houk and co-workers demonstrated[75] the powerful stereochemical control of dienophile heteroatom lone pairs in the DA reactions of formaldehyde, diazene, formaldimine, and nitrosylhydride with butadiene. These reactions have larger activation barriers than phosphaethene−butadiene cycloaddition since the C−N π bond (80.8 kcal/mol) is much stronger[74b,c] than C═P bond (49.4 kcal/mol). The ∼2 kcal/mol greater ΔE_{rxn} of the exo additions 3, 6, and 7 (Table 1), however, show that the product structures resulting from these exo reactions are thermodynamically more stable than those resulting from the endo additions.

Cossio et al. pointed out that although the transition state aromaticity was important, it does not determine

(75) McCarrick, M. A.; Wu, Y.; Houk, K. N. *J. Am. Chem. Soc.* **1992**, *114*, 1499.

SCHEME 4. NBO Bond Order of Reactants and TSs of DA Reactions of Ethene with Butadiene and Phosphethene with Butadiene and with Isoprene

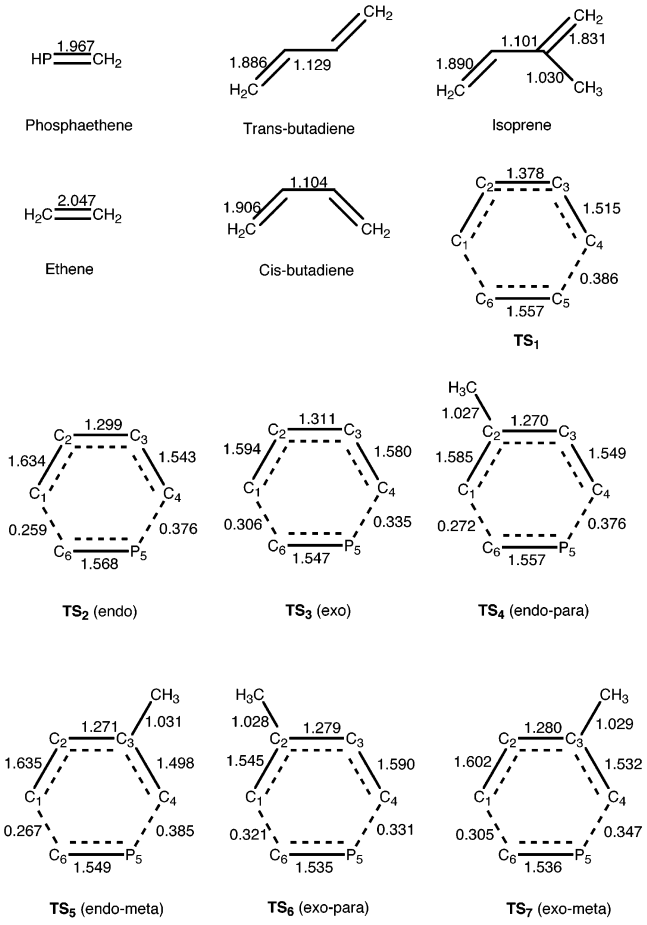

the regioselectivity of the reaction.[76b] In our cases, the energies of the alternative transition structures **TS$_4$** and **TS$_5$**, on one hand, and **TS$_6$** and **TS$_7$**, on the other, do not differ significantly. While **TS$_5$** and **TS$_7$**, which correspond to the preferred regioisomers, are lower in energy, the differences are only 0.16 and 0.35 kcal/mol, respectively.

Experimentally, DA reactions of isoprene with 2-acetyl-2*H*-1,2,3-diazaphosphole[23] and with 1,4,2-diazaphospholo-[4,5-*a*]pyridine[28] were reported to produce the meta regioproduct exclusively. To rationalize these results, we have computed the activation barriers for the concerted TSs of the DA reactions of isoprene with 2*H*-1,2,3-diazaphosphole (**10**), 2-acetyl-2*H*-1,2,3-diazaphosphole (**11**), 1,4,2-diazaphospholo[4,5-*a*]pyridine (**12**), and phosphacetylene (**13**). We have computed ΔE_a for the TSs for DA reactions resulting from exo and endo approaches of both reactants (reactions 8−19) as summarized in Table 2.

For comparison, we also computed the activation barriers of reactions 22 and 23, as well as those for the DA reaction of butadiene with acetylene (reaction 20) and with phosphacetylene (reaction 21).

The absolute energies and ZPE values of the reactants, products, and transition states are reported in Supporting Information (SI). The geometries of the reactants, TSs, and products, for all reactions (8 through 23), also are given in SI. Table 2 shows that the activation barriers (for the same dienophile) for exo and endo approaches of the reactants are quite similar. ΔE_{rxn} of these reactions (Table 2) are exothermic, except that reactions 8−11 become slightly endothermic when ZPE corrections ($\Delta E_{rxn + ZPE}$) are applied. ΔE_a and ΔE_{rxn} show that the TSs for the endo approach of the reactants for all reactions (8−19, in Table 2) are favored slightly (by about 0.3−0.9 kcal/mol) over those for the exo approach. The endo TSs are thus kinetically preferred.

The activation barriers (ΔE_a in Table 2) suggest that, for the endo approach of the reactants, TSs leading to meta products are preferred (by 0.7 kcal/mol) over TSs leading to para products. The same energetic preference for TSs leading to the meta product is found for the exo approach of the reactants. Similarly, the exothermicities (ΔE_{rxn} in Table 2) of reactions 8−19 show that meta products are preferred over para products, but only by about 0.2−0.7 kcal/mol. DA reactions of isoprene with phosphacetylene (reactions 22 and 23) also show that activation barriers leading to the meta product are only preferred slightly (0.2 kcal/mol) over those leading to para products. Also, the exothermicities of reactions 22 and 23 are almost the same. These isoprene reactions, 22 and 23, have activation barriers and exothermicities similar to that of butadiene reaction 21. As pointed out earlier, the presence of phosphorus in one of the reactants lowers the activation barrier as compared to that in the carbocyclic case, reaction 20.

The computed activation barriers and exothermicites of reactions 8−19 as well as 22 and 23 suggest that the experimentally observed regioselectivity of products cannot be accounted for by the closed shell pericyclic mechanism (concerted [4 + 2] DA cycloaddition). Also, reactions 12−19 would not proceed unless a small amount of catalyst is added. This provides a hint that another mechanism may be operative in such cases.

Radical Cation Reactions. It is known that radical cation DA reactions generally have low activation barriers but nevertheless show high regio- and stereoselectivities.[63] The dissociation of ionized cyclohexene into the butadiene radical cation and ethene, by field ionization mass spectrometry,[77,78] led to, in addition to the butadiene radical cation, other intermediates. These were generated by hydrogen scrambling, proposed to result from successive 1,3-allylic rearrangements. Hofmann and Schaefer investigated the reaction pathways connecting ethene and butadiene radical cation theoretically.[64] A stepwise addition involving an ion−molecule complex was involved, and the reaction was predicted to have a low activation barrier, only 6.3 kcal/mol. In addition, these authors investigated pathways besides addition of the butadiene radical cation to ethene leading to the DA product.[64]

We have investigated the radical cation pathway of phosphaethene with isoprene leading to the DA products, Chart 1. The geometries of all the intermediates and

(76) (a) Jiao, H.; Schleyer, P. v. R. *J. Phys. Org. Chem.* **1998**, *11*, 655. (b) Cossio, F. P.; Morao, I.; Jiao, H.; Schleyer, P. v. R. *J. Am. Chem. Soc.* **1999**, *121*, 6737.

(77) Bouchoux, G.; Salpin, J.-Y. *Rapid Commun. Mass Spectrom.* **1994**, *8*, 325.

(78) Derrick, P. J.; Fallick, A. M.; Burlingame, A. L. *J. Am. Chem. Soc.* **1972**, *94*, 6794.

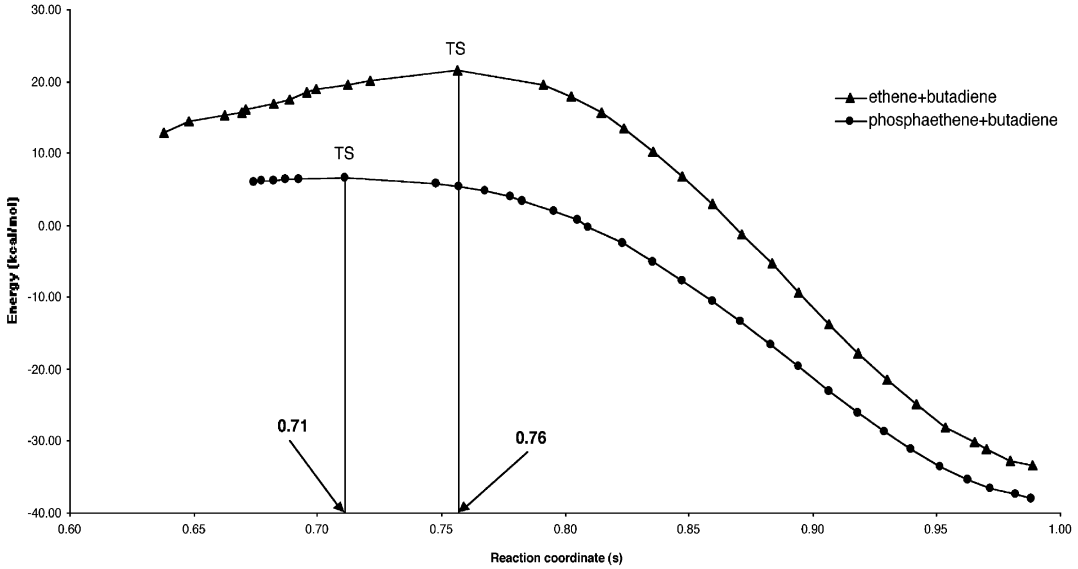

FIGURE 4. Intrinsic reaction coordinate (IRC) of [4 + 2] Diels−Alder reaction of butadiene with ethene and with phosphaethene at B3LYP/6-311+G** (for the definition of "s" refer to text).

TABLE 2. Activation Energies[a] (ΔE_a, kcal/mol), ZPE-Corrected Activation Energies[b] (ΔE_{a+ZPE}, kcal/mol), Exothermicities[a] (ΔE_{rxn}, kcal/mol) and ZPE-Corrected Exothermicities[b] ($\Delta E_{rxn+ZPE}$, kcal/mol) for DA Reactions of Isoprene (3) with 2*H*-1,2,3-Diazaphosphole (10; Reactions 8−11), with 2-Acetyl-2*H*-1,2,3-diazaphosphole (11; Reactions 12−15), with 1,4,2-Diazaphospholo[4,5-*a*]pyridine (12; Reactions 16−19), and with Phosphaacetylene (13; Reactions 22 and 23), and Also for the DA Reaction of Butadiene (2) with Acetylene (Reaction 20) and with Phosphacetylene (Reaction 21)

reaction no.	reaction	ΔE_a	ΔE_{a+ZPE}	ΔE_{rxn}	$\Delta E_{rxn+ZPE}$
8	**10** (endo) + **3** → **TS$_8$** → **14**-meta-endo	27.08	27.48	−2.40	0.42
9	**10** (endo) + **3** → **TS$_9$** → **15**-para-endo	27.73	28.19	−2.11	0.27
10	**10** (exo) + **3** → **TS$_{10}$** → **16**-meta-exo	26.87	27.38	−1.52	1.33
11	**10** (exo) + **3** → **TS$_{11}$** → **17**-para-exo	27.69	28.20	−1.77	0.98
12	**11** (endo) + **3** → **TS$_{12}$** → **18**-meta-endo	14.84	15.88	−16.91	−13.62
13	**11** (endo) + **3** → **TS$_{13}$** → **19**-para-endo	15.69	16.63	−16.71	−13.43
14	**11** (exo) + **3** → **TS$_{14}$** → **20**-meta-exo	15.43	16.30	−15.80	−12.47
15	**11** (exo) + **3** → **TS$_{15}$** → **21**-para-exo	16.67	17.58	−15.59	−12.25
16	**12** (endo) + **3** → **TS$_{16}$** → **22**-meta-endo	22.33	22.95	−11.80	−8.56
17	**12** (endo) + **3** → **TS$_{17}$** → **23**-para-endo	23.71	24.47	−11.14	−7.91
18	**12** (exo) + **3** → **TS$_{18}$** → **24**-meta-exo	23.00	23.49	−10.71	−7.52
19	**12** (exo) + **3** → **TS$_{19}$** → **25**-para-exo	23.71	24.31	−10.28	−7.02
20	acetylene + **2** → **TS$_{20}$** → **26**	25.65	27.40	−54.05	−47.47
21	**13** + **2** → **TS$_{21}$** → **27**	15.40	15.74	−35.41	−31.31
22	**13** + **3** → **TS$_{22}$** → **28**-meta	15.66	16.49	−36.12	−32.35
23	**13** + **3** → **TS$_{23}$** → **29**-para	15.84	16.67	−36.13	−32.44

[a] Relative energies at B3LYP/6-311+G**. [b] Relative energies at B3LYP/6-311+G** + ZPE (B3LYP/6-31G*).

TSs are displayed in Figure 5. For all reactions (24−27), our computations show that the highly reactive isoprene radical cation reacts with phosphaethene, without a barrier, to give a gauche-out intermediate (all attempts to locate a TS, leading to the gauche-out intermediate, at UHF/6-31G* and UB3LYP/6-31G* failed). This intermediate passes over a TS (rotation around the C−P bond) to give a gauche-in intermediate. The later intermediate then goes over another TS finally to give a DA cyclized radical cation product. As shown in Chart 1, the formation of the first intermediate, **int$_1$**, from isoprene radical cation and phosphaethene, is very exothermic for all reactions (24−27). Similarly, for all these reactions, the evolution of the DA-like radical cation products from the second intermediate, **int$_2$**, is also very exothermic, Chart 1. Note that all the energies in Chart 1 are relative to isoprene radical cation and phosphaethene.

Reactions 26 and 27, in Chart 1, have high barriers, ∼5.5 and ∼7.1 kcal/mol, respectively, for the formation of **int$_2$-in** from **int$_1$-out** as compared to that for reaction 25, 0.2 kcal/mol. Also, for reaction 24, barriers for the formation of **int$_2$** and of the radical cation product, 0.7 and 3.8 kcal/mol, respectively, are relatively higher than those needed for reaction 25, 0.2 and 3.4 kcal/mol. Thus reaction 25, leading to a meta-endo radical cation product, has negligible barriers along the reaction course and hence is the preferred pathway.

As evident from Chart 1 and Figure 5, the formation of **int$_2$** from **int$_1$** involves rotation around the C−P bond: surprisingly for the exo approach of the reactants, this barrier, **TS$_1$**, is higher. To investigate the origin of this high barrier, viz 5.5 kcal/mol, we have computed the DA reaction of butadiene radical cation with phosphaethene, Chart 2. For the exo addition of reactants,

CHART 1

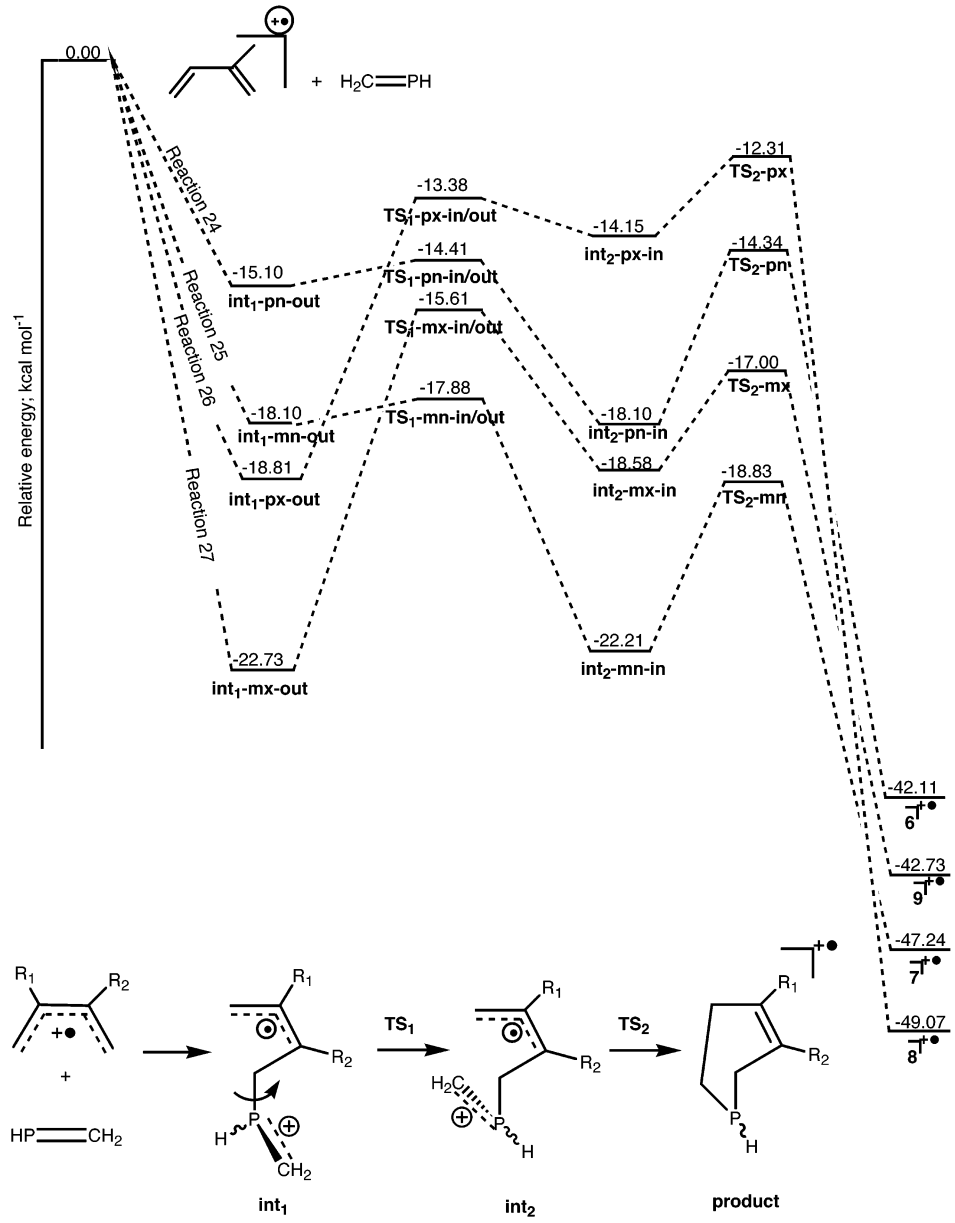

R_1=CH_3 and R_2=H reactions 24 and 26; R_1=H and R_2=CH_3 reactions 25 and 27

reaction 29 (the formation of the intermediate **int$_3$-exo-out**) is more exothermic (3.5 kcal/mol) than reaction 28 (**int$_3$-endo-out**). The population analysis (NPA), Chart 2, shows that charges in **int$_3$-exo-out** are more electronically delocalized, and hence this intermediate is preferred over **int$_3$-endo-out**. However, the barrier, 5.5 kcal/mol, for reaction 29 (exo addition), to form **TS$_3$**, is higher than that for reaction 28, 0.9 kcal/mol in Chart 2. The population analysis on these TSs shows that **TS$_3$-endo-in/out** is preferred because the charge is more delocalized over this structure as compared to that for **TS$_3$-exo-in/out**. Hence, the endothermicity is low for the formation of the former TS, **TS$_3$-endo-in/out**.

Aromaticity of the Concerted Transition States. Jiao and Schleyer[79] analyzed the aromaticity of pericyclic transition states systematically on the basis of geometric, energetic, and magnetic criteria. The aromatic transition structures exhibit exalted magnetic susceptibilities, magnetic susceptibility anisotropies, and abnormal ^{1}H NMR chemical shifts.

Schleyer et al.[60a] also developed a simple and effective criterion for determining the aromaticity of different systems, the nucleus independent chemical shifts (NICS), which is the negative of the computed magnetic shieldings at or above the ring centers. NICS, as an indicator of aromaticity, agrees well with the energetic, geometric, and magnetic criteria, in many related systems and does not require increment systems or other reference mol-

(79) (a) Jiao, H.; Schleyer, P. v. R. *Angew. Chem., Int. Ed. Engl.* **1993**, *32*, 1763. (b) Jiao, H.; Schleyer, P. v. R. *J. Chem. Soc., Perkin Trans. 2* **1994**, 407. (c) Herges, R.; Jiao, H.; Schleyer, P. v. R. *Angew. Chem., Int. Ed. Engl.* **1994**, *33*, 1376. (d) Jiao, H.; Schleyer, P. v. R. *J. Chem. Soc., Faraday Trans.* **1994**, *90*, 1559. (e) Jiao, H.; Schleyer, P. v. R. *J. Am. Chem. Soc.* **1995**, *117*, 11529. (f) Jiao, H.; Schleyer, P. v. R. *Angew. Chem., Int. Ed. Engl.* **1994**, *34*, 334.

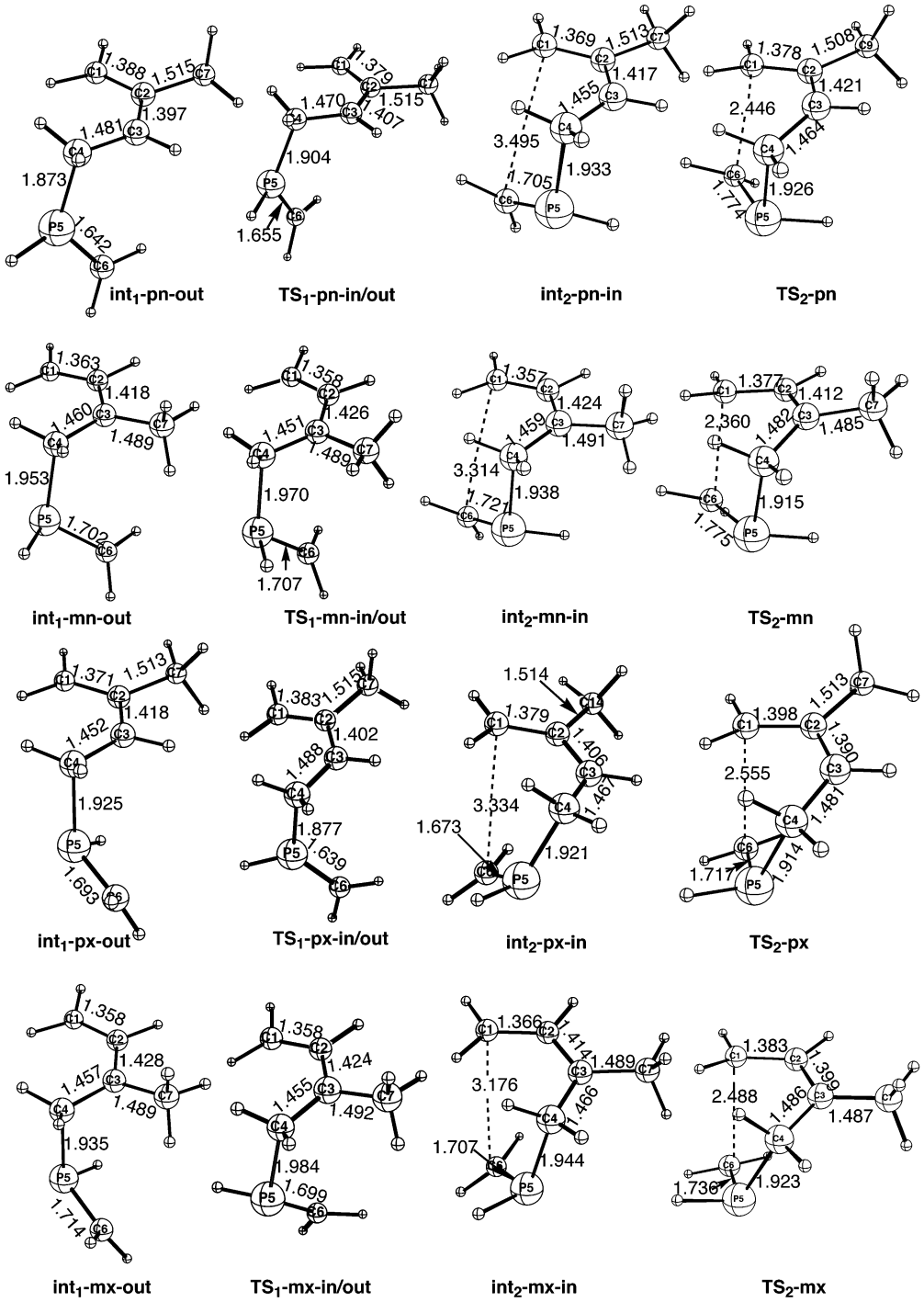

FIGURE 5. Optimized geometries (at UB3LYP/6-311+G**) of various stationary points and transition structures for the radical cation reaction of isoprene$^{+\bullet}$ with phosphaethene leading to DA radical cation products.

ecules (although comparisons are helpful for interpretation).[60c] NICS also is effective for assessing the aromaticity of the individual rings in polycyclic systems.[80] Cossio et al.[81] extended the NICS criterion to the characterization of in-plane aromaticity of the transition states in 1,3-dipolar cycloadditions. NICS values have also been used to determine the aromaticity and antiaromaticity of transition states.[76,82] As shieldings arise from the contributions of the core and various bonding electrons as well as from the mobile electrons (ring currents), we have used dissected NICS (separation of total NICS into π, σ, and core electron components inherent in the IGLO localization method) to evaluate

(80) (a) Jiao, H.; Schleyer, P. v. R. *Angew. Chem., Int. Ed. Engl.* **1996**, *35*, 2383. (b) Subramanian, G.; Schleyer, P. v. R.; Jiao, H. *Angew. Chem., Int. Ed. Engl.* **1996**, *35*, 2638.(c) Subramanian, G.; Schleyer, P. V. R.; Jiao, H. *Organometallics* **1997**, *16*, 2362. (d) Jiao, H.; Schleyer, P. v. R.; Mo, Y.; McAllister, M. A.; Tidwell, T. T. *J. Am. Chem. Soc.* **1997**, *119*, 6561. (e) Schleyer, P. v. R.; Manoharan, M.; Jiao, H.; Stahl, F. *Org. Lett.* **2001**, *3*, 3643.

(81) Lecea, B.; Morao, I.; Cossio, F. *J. Org. Chem.* **1997**, *62*, 7033.

(82) Sawika, D.; Houk, K. N. *J. Mol. Model.* **2000**, *6*, 158.

CHART 2

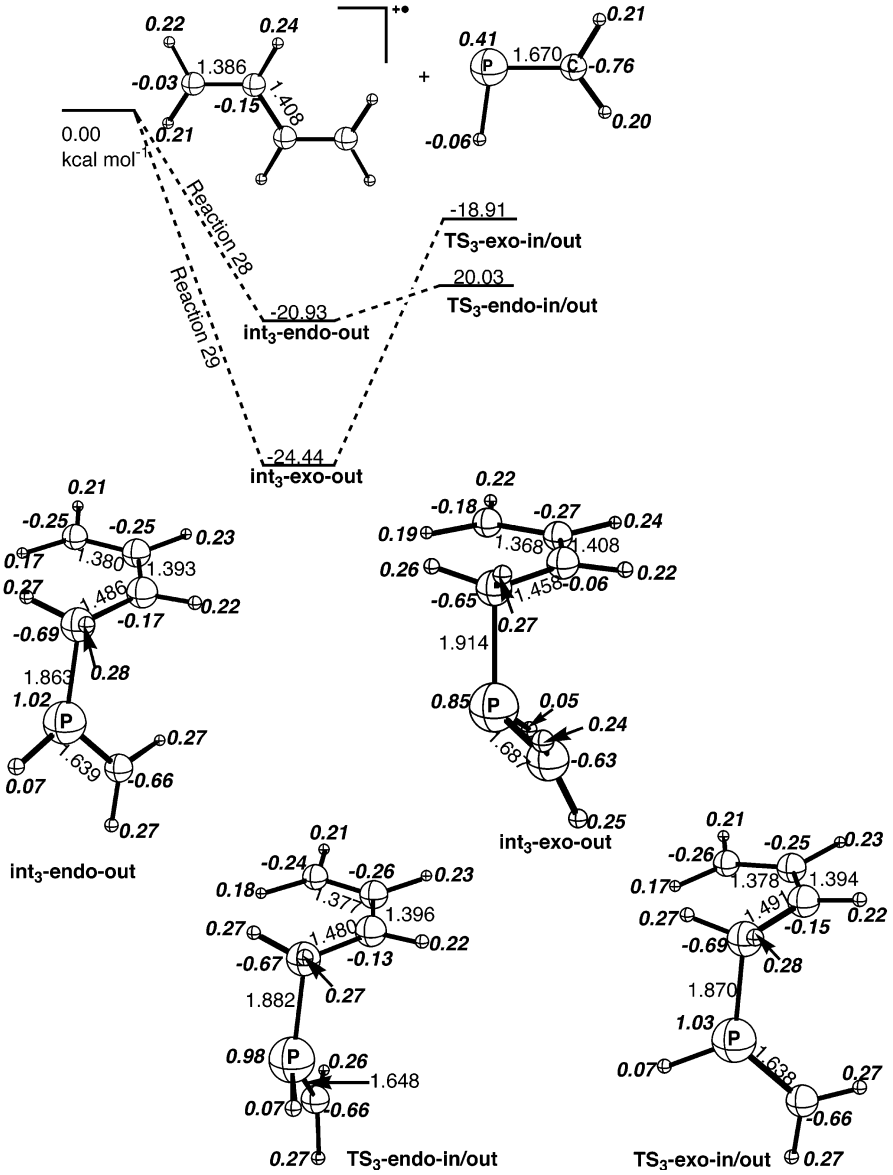

the delocalized electron contribution (aromaticity) to the total value.[60b,c]

A common difficulty in the calculation of magnetic properties is that gauge invariance is not guaranteed, i.e., the computational result may depend on the position of the molecule in the Cartesian frame. To overcome this problem, gauge-independent atomic orbital (GIAO) and individual gauge for localized orbital (IGLO) methods are employed. Unlike GIAO (a method in which each atomic orbital has its own local gauge origin), IGLO (localized molecular orbitals associated with individual gauge origins) gives an interpretative framework based on contributions from each localized orbital, e.g., lone pairs and core and bonding electrons. Since, Kutzelnigg's original IGLO program employed the Boys[83a] localization method (which represented double bonds by two equivalent τ (banana) orbitals), Pipek−Mezey localization, which provides π and σ separation,[83b] was employed here.

However, all localization schemes necessarily are arbitrary in treating inherently delocalized systems, like aromatic TSs. The nature of the localized orbitals, given by the program, sometimes seems counterintuitive. But the localization scheme generally reflects shorter distances and higher electron densities.

For example, **TS$_1$** in Figure 3 shows the localized structure of the synchronous TS for the cycloaddition of butadiene with ethene. The Pipek−Mezey localization of the six mobile electrons, shown by dotted lines, reflects the greater electron density in the C1−C2, C3−C4, and C6−C5 regions. This localized structure, **TS$_1$**, can be considered to be akin to a "resonance hybrid" of the TS (Scheme 5). The cyclic six electron delocalization, **a**, can be represented in terms of such resonance hybrids involving **b** and **c**. The resonance hybrid weights of these competing structures can be evaluated by the NBO program.[84] One of the later pair, **c**, is chosen by the Pipek−Mezey localization scheme because the C1−C2 and C5−C6 distances are shorter than the C2−C3 and

(83) (a) Foster, S.; Boys, S. F. *Rev. Mod. Phys.* **1960**, *32*, 296, 303, 305. (b) Pipek, J.; Mezey, P. G. *Chem. Phys.* **1989**, *90*, 4916.

SCHEME 5

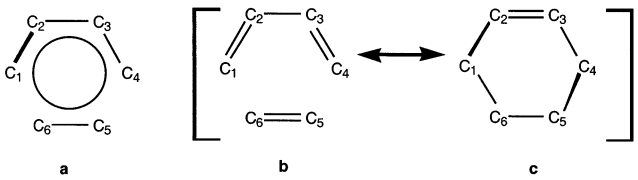

C1–C6 distances. In the IGLO output, one can differentiate σ bonds from the mobile electrons (or π bonds) by analyzing the shielding tensors. Generally, σ bonds have small shielding tensors for in-plane (σ_{xx} and σ_{yy}) and out-of-plane (σ_{zz}) components, whereas mobile electrons have large out-of-plane shielding tensors, σ_{zz} (and small σ_{xx} and σ_{yy}).

Table 3 compares NICS values at the geometrical heavy-atom centers of TSs. NICS given by the GIAO and IGLO methods agree. **TS$_2$**–**TS$_7$** have large negative NICS (from −16.8 to −17.2). The NICS values suggest strong ring currents in the TSs. The NICS values for **TS$_2$**–**TS$_7$** are slightly lower than that in the parent DA reaction **TS$_1$**. Additionally, the dissected NICS (Table 3) at the centers of **TS$_2$**–**TS$_7$** show diatropic contributions (from −11.8 to −13.4) from six mobile electrons. Thus, the dissected NICS values also confirm the aromaticity of these TSs. The contributions from the six mobile electrons in **TS$_2$**–**TS$_7$** are less than −20.7 for benzene and less than −14.0 for **TS$_1$**. This decrease in the six mobile electron contributions indicates a smaller ring current than that in benzene.

The calculated ^{1}H NMR chemical shifts of the reactants are in good agreement with the experimental values.[85] The changes observed in the NMR chemical shifts of the terminal protons of the diene along the reaction path are of particular interest.[79c] The outer protons on C1 and C4 (in **TS$_2$**–**TS$_7$**) are only slightly downfield, from 5.5 to 6.3 ppm, as compared to those in 1,3-butadiene, 5.2 ppm. However, the inner protons of C_1 and C_4 (in **TS$_2$** through **TS$_7$**), from 0.7 to 1.2 ppm, show large upfield shifts compared to the reactants, 5.9 ppm (Figures 1 and 3). The ^{1}H NMR chemical shifts of these inner protons fall in the range expected for a nonaromatic ring in the products, Figure 2. On the other hand, chemical shifts of protons attached to C_2 and C_3 do not change much along the reaction path and in the products have values expected for vinylic protons. The proton attached to P experiences large changes in chemical shift along the reaction path and is also affected by the (exo and endo) approach of the two reactants. As expected, from its inner location, this δ H is more upfield, about 0.7–0.8 ppm, in the transition state resulting from the endo approach but is in the range for protons bound to tricoordinate phosphorus in the products. The inner proton attached to C6, in **TS$_2$**–**TS$_7$**, is also shifted upfield, from 3.1 to 5.1 ppm, as compared to 8.7 ppm, in the phosphaethene. Thus, all "inner" protons on both diene as well as dienophile show pronounced chemical shifts due to electronic effects arising from delocalization.

TABLE 3. Computed Magnetic Susceptibility Exaltations (Λ, cgs ppm), GIAO–NICS(0) at the Center of the TS and Six Mobile Electron Contributions to Dissected NICS for Reactions between Phosphaethene 1 and 1,3-Dienes 2 and 3

reaction	Λ[a]	GIAO–NICS(0)[b] (IGLO–NICS(0))[c]	mobile electron contribution to IGLO–NICS[c]
benzene	−15.76	−8.0 (−8.8)	−20.7
1	−19.3	−18.5 (−19.4)	−14.0
2	−24.7	−17.0 (−18.0)	−12.5
3	−24.3	−16.8 (−17.7)	−13.0
4	−23.9	−17.2 (−18.0)	−12.8
5	−23.0	−16.8 (−17.7)	−12.7
6	−22.7	−17.0 (−17.7)	−13.4
7	−22.8	−17.0 (−17.7)	−13.1

[a] Magnetic susceptibility exaltations at B3LYP/6-31+G*//B3LYP/6-311+G**. [b] NICS(0) at GIAO–B3LYP/6-31+G*//B3LYP/6-311+G**. [c] Dissected NICS using the deMon-Master NMR program, SOS-DFPT, with the Perdew-Wang-91(PW91) exchange correlation functional and the IGLO-III TZ2P basis set (recommended options).

Jiao and Schleyer[79a,c] also applied magnetic susceptibility exaltation criteria to demonstrate the cyclic delocalization in pericyclic TSs. The calculated total magnetic susceptibility (including paramagnetic, diamagnetic, and nonlocal contributions) for such TSs is quite different from that of the reactants. This difference was taken to be the magnetic susceptibility exaltation of the TSs. The magnetic susceptibility exaltations (ranging from −22.7 to −24.7 cgs ppm, Table 3) for **TS$_2$**–**TS$_7$** are higher than −19.3 cgs ppm, for **TS$_1$**, and are also higher than −15.7 cgs ppm, for benzene. Thus, the magnetic susceptibility exaltation values of **TS$_2$**–**TS$_7$** also demonstrate the aromaticity of these TSs.

Conclusions

The [2 + 4] cycloadditions of phosphaethene with 1,3-dienes occur via aromatic transition structures. The ^{1}H NMR chemical shifts, magnetic susceptibility exaltations, and NICS values at the center of these asynchronous TSs show the presence of ring currents circulating along the molecular perimeters. Evaluations of the bond orders of all the TSs (**TS$_1$** and **TS$_2$**–**TS$_7$**) as well as IRC suggest that TSs resulting from DA reactions of phosphaethene with butadiene and with isoprene are earlier than the **TS$_1$** of the parent DA reaction. Hence, the activation barriers for forming **TS$_2$**–**TS$_7$** of phosphaethene–butadiene or isoprene, are much lower than that needed for forming the parent DA **TS$_1$**. However, the exothermicities of phosphethene cycloadditions with butadiene or with isoprene and the DA of butadiene with ethene are in the same range.

The computed regioselectivities of the products for reactions 4–7 (cycloaddition of phosphaethene with isoprene) are all quite low: the differences in the barriers leading to regioisomeric products are less than 0.4 kcal/mol. Computational investigations of the DA reactions of isoprene with 2*H*-1,2,3-diazaphospholes, 2-acetyl-2*H*-

(84) Information available at http://www.chem.wisc.edu/~nbo5/tut_nrt.htm, NRT Transition State Analysis assessed on December 15, 2001.

(85) (a) Pouchert, C. J.; Campbell, J. R. *The Aldrich Library of NMR Spectra*; Aldrich Chemical Co.: Milwaukee, 1974. (b) *High Resolution NMR Spectra Catalogue;* Varian Associates, 1964. (c) Bovey, F. A. *NMR Data Tables for Organic Compounds*; Wiley-Interscience: New York, 1967. (d) Wiberg, K. B.; Nist, B. J. *The Interpretation of NMR Spectra*; Benjamin: New York, 1962. (e) Sasaki, S. *Handbook of Proton-NMR Spectra and Data*; Academic Press: New York, 1985. (f) Silverstein, R. M.; Bassler, G. C.; Morill, T. C. *Spectrometric Identification of Organic Compounds*; Wiley and Sons: New York, 1991.

1,2,3-diazaphosphole, 1,4,2-diazaphospholo[4,5-*a*]pyridine, and phosphacetylene show that the regioisomeric (meta and para) products should be formed in roughly 2:1 ratios. In contrast, experimentalists failed to detect the para regioisomer (such conclusions were based on the presence of only one ^{31}P NMR signal in the products).[23] In addition, it was reported that the reaction could not proceed without adding catalysts.

A mechanistic alternative, computations on a stepwise addition of isoprene radical cation with phosphaethene, shows that TSs leading to meta-endo radical cation product have negligible barriers along the reaction course and hence would be the preferred pathway.

In conclusion, computations of the activation barriers of the TSs for the concerted DA reactions of isoprene with phosphaethene (reactions 4−7) and other dienophiles (reactions 8−23) do not account for the regioselectivity of products observed experimentally in some reactions. High regioselectivities, e.g., of reactions 8−19, might result via a radical cation mechanism.

Acknowledgment. R.K.B. would like to thank the Alexander von Humboldt Foundation for supporting his visit to the Computational Chemistry Center, University of Erlangen, Germany, where the initial computations were carried out. We also would like to thank Dr. Y. Yamaguchi and Dr. M. Manoharan for helpful discussions.

Supporting Information Available: Table A, containing the absolute energies (at B3LYP/6-311+G**) and unscaled zero point energy corrections (at B3LYP/6-31G*); Table B, containing the Cartesian coordinates of reactants, products, transitions states, and intermediates of reactions 1−29; Figure A, containing optimized geometries of TSs; and Figure B, containing optimized geometries of reactants and products resulting from reactions 8−27. This material is available free of charge via the Internet at http://pubs.acs.org.

JO026284I